Catalytic Combustion Kinetics of Isopropanol over Novel Porous Microfibrous-Structured ZSM-5 Coating/PSSF Catalyst

Huanhao Chen, Ying Yan, Yan Shao, and Huiping Zhang
School of Chemistry and Chemical Engineering, South China University of Technology, Guangzhou 510640, P.R. China

Huanhao Chen
Dept. of Chemical Engineering, University of Puerto Rico-Mayagüez Campus, Mayagüez, Puerto Rico 00681-9000

DOI 10.1002/aic.14670
Published online November 11, 2014 in Wiley Online Library (wileyonlinelibrary.com)

Porous thin-sheet cobalt–copper–manganese mixed oxides modified microfibrous-structured ZSM-5 coating/PSSF catalysts were developed by the papermaking/sintering process, secondary growth process, and incipient wetness impregnating method. Paper-like sintered stainless steel fibers (PSSF) support with sinter-locked three-dimensional networks was built by the papermaking/sintering process, and ZSM-5 coatings were fabricated on the surface of stainless steel fibers by the secondary growth process. Catalytic combustion performances of isopropanol at different concentrations over the microfibrous-structured Co–Cu–Mn (1:1:1)/ZSM-5 coating/PSSF catalysts were measured to obtain kinetics data. The catalytic combustion kinetics was investigated using power–rate law model and Mars–Van Krevelen model. It was found that the Mars–Van Krevelen model provided fairly good fits to the kinetic data. The catalytic combustion reaction occurred by interaction between isopropanol molecule and oxygen-rich centers of modified microfibrous-structured ZSM-5 coating/PSSF catalyst. The reaction activation energies for the reduction and oxidation steps are 60.3 and 57.19 kJ/mol, respectively. *AIChE J*, 61: 620–630, 2015
Keywords: catalysis, fibers, kinetic model, isopropanol, ZSM-5 coating

Introduction

Volatile organic compounds (VOCs) such as isopropanol have always been considered to be a major source of air pollutants, emitting from many industrial fields, and transportation processes.[1–5] Over the past decades, catalytic combustion has been recognized as one of the most promising techniques for the elimination of VOCs from gaseous streams due to its relatively higher efficiency and lower energy consumption.[6–13]

The widely used supported transition metal oxides (such as cobalt,[14–17] copper,[13,18–22] manganese[6,7,23–27]) catalysts are most active for the catalytic combustion of VOCs in air. However, the traditional fixed bed reactors packed with catalyst particulates with large particle sizes always suffer from poor mass/heat transfer efficiency, low contacting efficiency, fluid bypassing, and relatively higher bed pressure drop.[28] Hence, it is important to develop novel structured catalyst materials for designing a highly efficient catalytic combustor, obviously improving the mass/heat transfer and contacting efficiency. A new class of composite materials fabricated by wet lay-up papermaking/sintering process can incorporate ZSM-5 zeolite coating with thickness as small as 4 μm onto the surface of stainless steel fibers.[29–31] The porous thin-sheet ZSM-5 coating/PSSF (paper-like sintered stainless steel fibers [PSSF]) with uniform microfibrous structure possesses a perfect combination of large void volume, uniform micropore structure, entirely open structure, high thermal conductivity, and permeability.[29–33] The ZSM-5 coating/PSSF composite, an excellent catalyst support permits advanced design of catalytic structured reactors with many beneficial properties that can effectively solve the problems encountered in traditional fixed bed reactors.[33] Our previous catalytic structured reactors based on mixed transition metal oxides modified microfibrous-structured ZSM-5 coating/PSSF catalysts can offer a much higher catalytic activity, excellent reaction stability, higher mass/heat transfer efficiency and contacting efficiency, and relatively lower bed pressure drop.[32,33]

The development of a suitable kinetic model for catalytic combustion of VOCs represents a key element in the prediction of the reaction mechanism.[1,34–36] The catalytic combustion kinetics must be taken into account for designing a reliable catalytic combustion reactor and improving the catalytic combustion performance of the existing catalyst.[34] The catalytic combustion kinetics of VOCs over various traditional fixed bed reactors packed with various catalysts has been presented in the literature.[34,35,37–42] Abdullah et al.[1] investigated the kinetic study of catalytic combustion of

Additional Supporting Information may be found in the online version of this article.

Correspondence concerning this article should be addressed to Y. Yan at yingyan@scut.edu.cn.

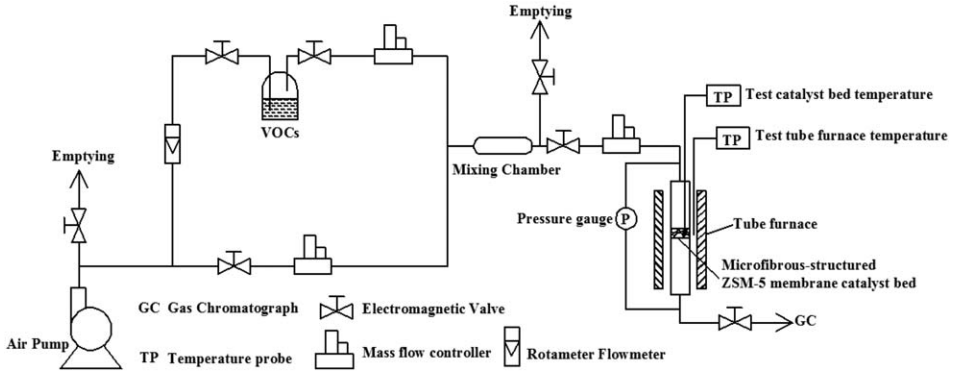

Figure 1. A schematic diagram of the catalytic combustion test setup.

ethyl acetate and benzene in air stream over Cr-ZSM-5 catalyst using several kinetic models. They found that the catalytic combustion kinetic data of VOCs over metal-exchanged zeolites were best fitted by the Mars–Van Krevelen model. He et al.[36] have also evidenced that the Mars–Van Krevelen model can accurately predict the catalytic combustion kinetics of VOCs over Pd/ZSM-5 catalysts. However, no reports are available on the catalytic combustion kinetics of VOCs in catalytic structured reactor with mixed transition metal oxides modified microfibrous-structured ZSM-5 coating/PSSF catalysts. Thus, the development of suitable kinetic model with more insights into the catalytic combustion reaction mechanism of VOCs over the porous mixed transition metal oxides modified microfibrous-structured ZSM-5 coating/PSSF catalysts is a worthwhile effort.

The aim of this work is to investigate the catalytic combustion kinetics of isopropanol over the porous thin-sheet cobalt–copper–manganese mixed oxides modified microfibrous-structured ZSM-5 coating/PSSF catalysts.

Experimental

Preparation of modified microfibrous-structured ZSM-5 coating/PSSF catalyst

Novel porous thin-sheet ZSM-5 coating/PSSF composites were prepared by the wet lay-up papermaking process and secondary growth process according to our previous reports.[29,30] The detailed procedure for producing the porous PSSF by the wet lay-up papermaking/sintering process is described as following: 6 g of stainless steel fibers (6.5 μm in diameter, 2–3 mm length) and 3 g of cellulose fibers were added to water and stirred vigorously to form a uniform suspension. A circular precursor paper was prepared by filtering the uniform suspension using wet lay-up process. The dried precursor paper was allowed to sinter in a flow of N_2 at 1050°C for 30 min to destroy the cellulose and form a porous thin-sheet PSSF support. The ZSM-5 coatings were fabricated on the surface of stainless steel fibers by secondary growth process. The silicalite-1 seeds solution was prepared by hydrothermal synthesis method using the synthesis solution with a molar ratio $9TPAOH/25TEOS/500H_2O/100C_2H_5OH$.[43] The PSSF was then treated with silicalite-1 seeds solution to adsorb a silicalite-1 seeds film on the surface of stainless steel fibers. During secondary growth process, the ZSM-5 zeolite coatings were fabricated on the surface of stainless steel fibers using secondary synthesis solution with a molar composition $1SiO_2/0.112TPAOH/0.008Al_2O_3/111H_2O$.[44] The ZSM-5 zeolite coatings were also synthesized at different crystallization temperatures (120–170°C) for 48 h. The resulting porous thin-sheet ZSM-5 coating/PSSF was incipiently impregnated with an aqueous solution containing appointed amount of $Co(NO_3)_2$, $Cu(NO_3)_2$, and $Mn(NO_3)_2$ with Co/Cu/Mn molar ratio of 1/1/1. The as-synthesized samples were dried at 100°C for 12 h and calcined at 350°C for 6 h to obtain the porous Co–Cu–Mn mixed oxides modified microfibrous-structured ZSM-5 coating/PSSF catalysts with a total metal loading of 28 wt %.

Characterization

The morphologies of the catalysts were observed by scanning electron microscopy (SEM, Hitachi S-3700N). The energy dispersive X-ray spectrometer (EDS) mapping images of the catalysts were also measured by EDS (Quantax, Bruker Co., Germany) coupled with a microscope chamber. X-ray diffraction (XRD) patterns of catalysts were recorded on a D8 Advance (Bruker Co.) diffractometer using Cu Kα radiation (40 kV, 40 mA) with 2θ range of 5–80°. The X-ray tube was operated at 40 kV and 40 mA. N_2 adsorption/desorption isotherms of catalysts were tested using an ASAP 2020 (Micromeritics Instrument Co.), GA at 77 K. The X-ray photoelectron spectra (XPS) results were obtained by a Kratos Axis Ultra Delay Line Detector (DLD) spectrometer with an Al Kα (1486.6 eV) radiation source operated at 15 kV and 10 mA. The binding energy of C1s peak at 284.6 eV was taken as a reference. Temperature programmed reduction (TPR) tests were tested on a Quantachrom Automated Chemisorption Analyzer. Fifty milligrams of each sample was loaded into the reactor and purged with 30 mL/min of helium at 300°C for 1 h to eliminate contaminants, and then cooled down to room temperature. The temperature was increased to 700°C at a heating rate of 10°C/min in a flow of 10% H_2 and 90% Ar.

Catalytic test

Catalytic combustion tests were carried out in a continuous flow experimental apparatus shown in Figure 1 at atmospheric pressure. As depicted in Figure 2, the catalytic structured reactor used in this study filled with microfibrous-structured ZSM-5 coating/PSSF catalysts consists of a 10 mm i.d stainless steel tube placed inside a tube furnace and a catalyst bed of 1 cm height. The temperature of the microfibrous-structured ZSM-5 coating/PSSF catalyst bed and the tube furnace was monitored automatically by E-type

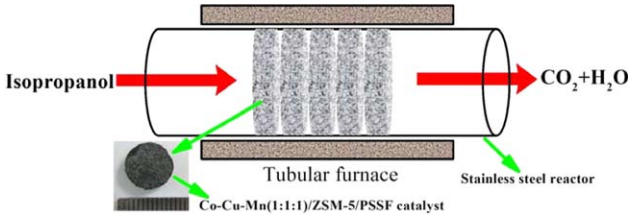

Figure 2. Schematic of the catalytic structured reactor based on Co–Cu–Mn (1:1:1)/ZSM-5 coating/PSSF catalysts used in this work for catalytic combustion of isopropanol in the air.

[Color figure can be viewed in the online issue, which is available at wileyonlinelibrary.com.]

thermocouples, respectively. The temperatures at the different positions of the catalyst bed were almost equal due to the high thermal conductivity properties of microfibrous-structured ZSM-5 coating/PSSF catalysts (See Figure S10 in Supporting Information). Therefore, the temperature at the middle of the catalyst bed was selected as the reaction temperature. The vapor of isopropanol was generated by passing air at a certain flow rate through the generator, containing 2.1–9.5 mg/L of isopropanol in air. For each experimental condition, the reaction was allowed to reach a steady state by waiting for 20 min, and the feed and effluent streams were analyzed on-line using gas chromatographs (Agilent 7890A, Palo Alto, CA) equipped with FID and TCD detectors for the quantitative analysis of the reactants and products. The data were the average of at least three measurements. In this work, the only final products were CO_2 and H_2O and no other by-products were observed under the experimental conditions. Before each series of tests, blank tests showed that no homogeneous reactions took place in the gas phase under the experimental conditions. All the catalytic combustion kinetics experiments of isopropanol over catalytic structured reactor were measured under oxygen-rich conditions (300.1 mg/L in the feed gas) and kinetics data were calculated using the conversions below 25%.[45]

The conversion (X_{iso}, %) and reaction rate ($-r_i$) of isopropanol over the catalytic structured reactor were calculated as follows

$$X_{iso} = \frac{C_{iso,in} - C_{iso,out}}{C_{iso,in}} \times 100\% \quad (1)$$

$$-r_i = \frac{F_{iso,in} X_{iso}}{V_{cat}} \quad (2)$$

where $C_{iso,in}$ (mg/L) and $C_{iso,out}$ (mg/L) are the inlet and outlet concentrations of isopropanol, respectively. $F_{iso,in}$ is the inlet molar flow rate of isopropanol (mol/s), and V_{cat} is the volume of the catalyst (cm^3).

Results and Discussion

Materials characterization

Figure S1a–d in Supporting Information present the photographs and SEM surface morphologies of PSSF support. Clearly, the wet lay-up papermaking/sintering process led to a three-dimensional (3-D) network with the large void volume and entirely open macroscopic structures. Figure S1e and f show that the silicalite-1 seeds layer covered on the surface of stainless steel fibers is uniform and the size of seeds is about 200 nm. From the SEM cross-sectional images in Figure 3, after application of the secondary growth process for various crystallization times, the thickness of the ZSM-5 coatings synthesized at 150°C after 12, 24, 48, 72, and 96 h is 0.6, 2.5, 4.0, 4.5, and 5.0 μm, respectively. It can be seen that the ZSM-5 coatings with different thickness can be fabricated on the surface of stainless steel fibers by varying the crystallization time. As can be seen in Figure 4, the ZSM-5 coatings synthesized at different crystallization temperatures are continuous. The ZSM-5 coatings with different zeolite particle sizes can be obtained by varying crystallization temperatures. The XRD patterns of ZSM-5 coatings synthesized at different crystallization temperatures are presented in Figure 5. The ZSM-5 coatings exhibit several typical diffraction peaks at $2\theta = 7–9°$ and 23–25°, matching well with the standard pattern of ZSM-5 zeolite.[46] The intensities of typical diffraction peaks of ZSM-5 coatings increase with increase in crystallization temperature, matching well with the SEM measure results in Figure 4. The diffraction peaks at $2\theta = 43–45°$ are attributed to the stainless steel fibers.

The resulting porous thin-sheet ZSM-5 coating/PSSF supports with different coating thickness and zeolite particle sizes were impregnated with an aqueous solution containing appointed amount of $Co(NO_3)_2$, $Cu(NO_3)_2$, and $Mn(NO_3)_2$ with Co/Cu/Mn molar ratio of 1/1/1. The total metal loading of Co–Cu–Mn mixed oxides modified microfibrous-structured ZSM-5 coating/PSSF catalysts was 28 wt %. Figure S2 in Supporting Information shows the SEM surface images and photograph of cobalt–copper–manganese mixed oxides modified microfibrous-structured ZSM-5 coating/

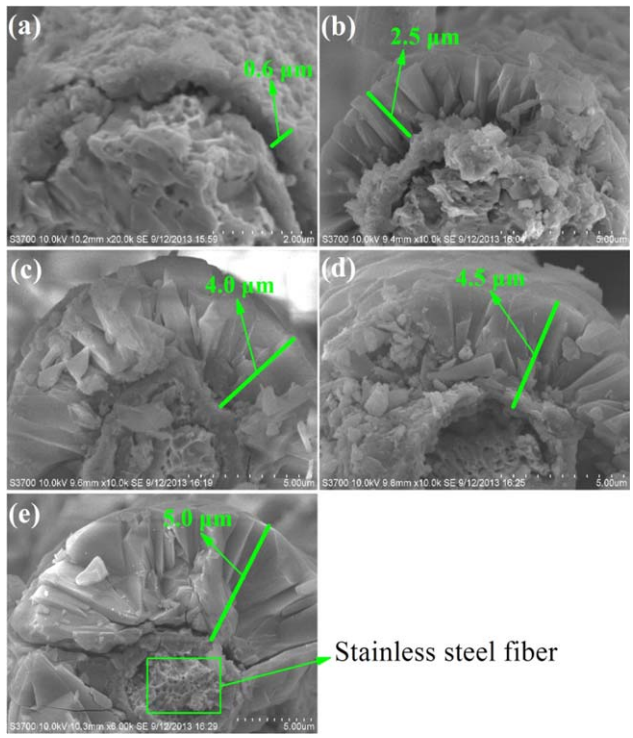

Figure 3. SEM cross-sectional images of ZSM-5 coatings covered on the stainless steel fibers surface after secondary growth for 12 h (a), 24 h (b), 48 h (c), 72 h (d), and 96 h (e).

[Color figure can be viewed in the online issue, which is available at wileyonlinelibrary.com.]

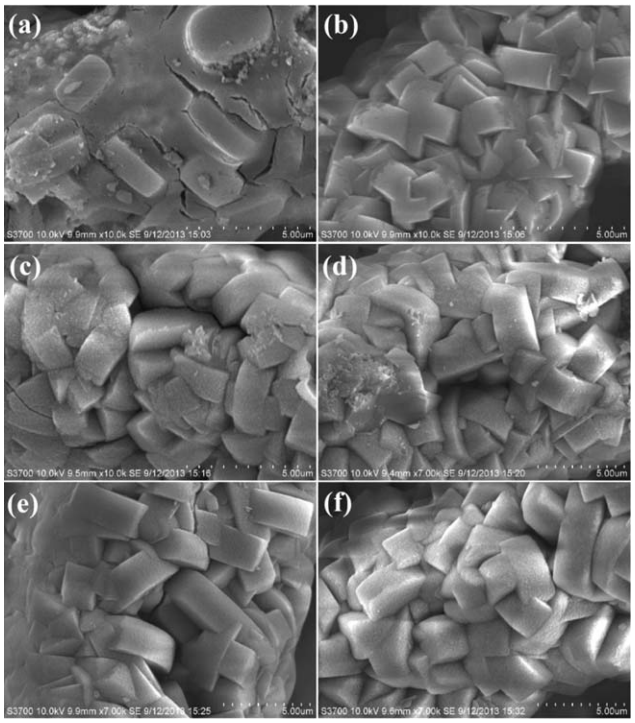

Figure 4. SEM surface micrographs of ZSM-5 coatings covered on the stainless steel fibers surface synthesized at different crystallization temperatures: 120°C (a), 130°C (b), 140°C (c), 150°C (d), 160°C (e), and 170°C (f).

PSSF catalyst (the ZSM-5 coating synthesized at 150°C for 48 h, total metal loading of 28 wt %). From the SEM top views in Figure S2c, the cobalt–copper–manganese mixed oxides spread well over the surface of ZSM-5 coating. The EDS elemental analysis spectra (Supporting Information, Figure S3) and mapping images (Supporting Information, Figure S4), XRD pattern (Supporting Information, Figure S5), H_2-TPR performance (Supporting Information, Figure S6), $N2_2$ adsorption–desorption isotherm (Supporting Information, Figure S7, Table S1), and XPS results (Supporting Information, Figure S8, Table S2) of Co–Cu–Mn (1:1:1)/ZSM-5 coating/PSSF catalyst are also clearly presented in the Supporting Information. All the detailed analysis results of Co–Cu–Mn (1:1:1)/ZSM-5 coating/PSSF catalyst can be found in our previous report.[32] The resulting catalysts with unique microfibrous structure possess a perfect combination of large void volume, uniform micropore structure, entirely open structure, high thermal conductivity and permeability, thereby leading to a good catalytic activity for isopropanol combustion.

Study of mass transfer limitations and thermal effects

It is well known that the catalytic combustion kinetic tests must be carried out in the absence of mass transfer and thermal effects.[36] Mass transfer limitations were tested by conducting catalytic combustion experiments at the reaction temperature of 220°C (Inlet concentration of isopropanol is 3.7 mg/L, concentration of oxygen is 300.1 mg/L). The external mass transfer effects were studied by carrying out catalytic combustion experiments of isopropanol over the catalytic structured reactor based on Co–Cu–Mn (1:1:1)/ZSM-5 coating/PSSF catalysts with bed height of 1 cm (the ZSM-5 coating synthesized at 150°C for a crystallization period of 48 h, the catalyst with a total metal loading of 28 wt % synthesized at a calcination temperature of 350°C) by varying the gas hourly space velocity (GHSV) from 7643 to 53,503 h^{-1}. Figure 6a shows that the isopropanol conversions in the GHSV range of 30,573–53,503 h^{-1} are essentially the same, indicating the absence of external mass transfer limitations for the catalytic combustion kinetics experiments under the present conditions. The possible explanation is that the sintered stainless steel fibers with a 3-D network offer the large void volume and entirely open macroscopic structures. Therefore, a GHSV of 30,573 h^{-1} was chose for the catalytic combustion kinetics experiments to avoid external mass transfer limitations. The internal mass transfer effects were examined by carrying out catalytic combustion experiments of isopropanol at a constant GHSV of 30,573 h^{-1} over the catalytic structured reactor with a bed height of 1 cm (the ZSM-5 coatings with different thickness and zeolite particle sizes, and a total metal loading of 28 wt %). As shown in Figures 3 and 4, the ZSM-5 coatings with different thickness or zeolite particles sizes can be fabricated by varying crystallization time and crystallization temperature. It can be seen from Figure 6b and c that no prominent difference in the conversion of isopropanol was observed for the modified microfibrous-structured ZSM-5 coating catalysts with different coating thickness or zeolite particles sizes. The possible reasons are that the ZSM-5 coating can offer high contacting efficiency, and have relatively lower internal mass transfer resistance, and shorter diffusion path due to their uniform micropore structures, small coating thickness, and zeolite particles sizes on micron scale. Therefore, the Co–Cu–Mn (1:1:1)/ZSM-5 coating/PSSF catalyst (the ZSM-5 coating synthesized at 150°C with a crystallization period of 48 h, the catalyst with a total metal loading of 28 wt % synthesized at a calcination temperature of 350°C) was used for conducting kinetics experiments of isopropanol over the catalytic structured reactor. According to previous reports,[34,36,38] for lower isopropanol conversions (less than

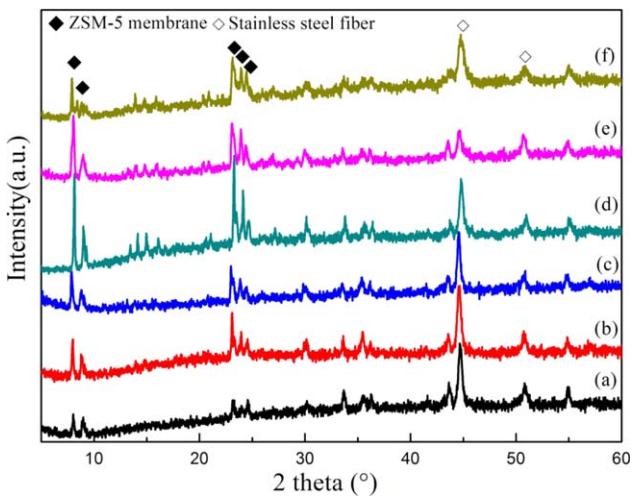

Figure 5. XRD patterns of ZSM-5 coatings covered on the stainless steel fibers synthesized at different crystallization temperatures: 120°C (a), 130°C (b), 140°C (c), 150°C (d), 160°C (e), and 170°C (f).

[Color figure can be viewed in the online issue, which is available at wileyonlinelibrary.com.]

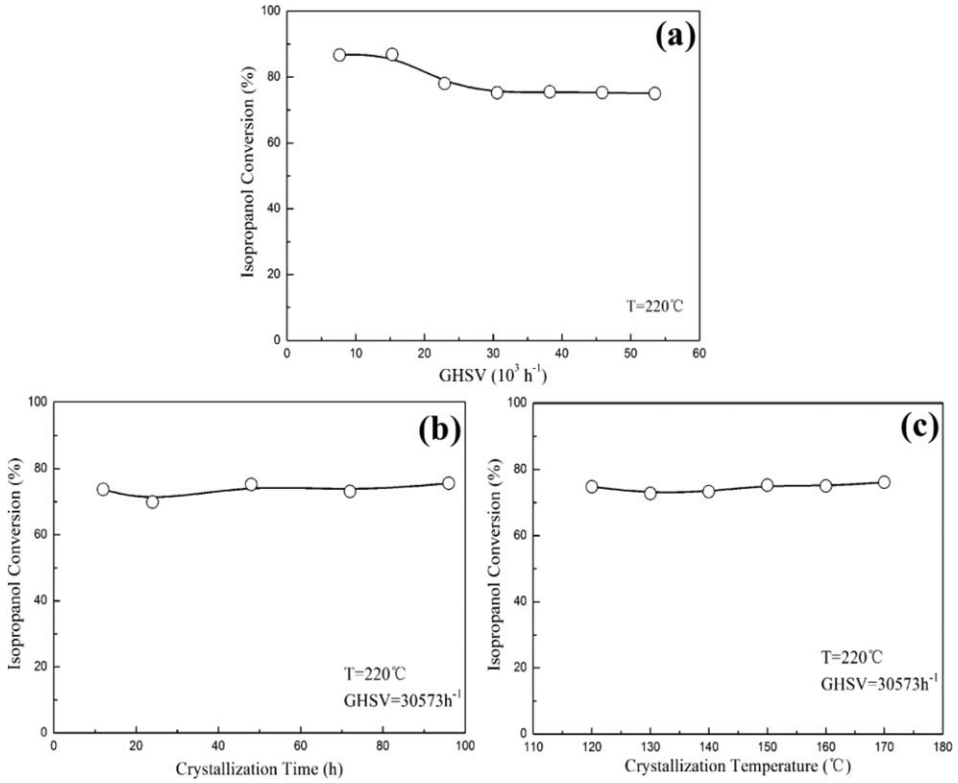

Figure 6. The evaluation results of mass transfer limitations: (a) evaluation of the external diffusion effect; (b) and (c) evaluation of the internal diffusion effect.

25% in this study), thermal effects in catalytic combustion reactions can be neglected for reactors with small inner diameter (around 9 mm) and relatively higher gas velocity ($>1 \times 10^4$ h^{-1}). The reactor used in this study has an inner diameter of 10 mm. Thermal conductivity properties of the microfibrous-structured ZSM-5 coating/PSSF catalyst were also provided in the Supporting Information. It can be seen in Supporting Information, Figure S10 that the surface of microfibrous-structured ZSM-5 coating/PSSF catalyst heated at 150°C presents a relatively uniform color, indicating that the microfibrous-structured ZSM-5 coating/PSSF catalyst exhibits excellent heat transfer properties and thermal conductivity. The microfibrous-structured ZSM-5 coating/PSSF catalyst possesses a high thermal conductivity due to the metallic nature, the stainless steel fibers have a high thermal conductivity [around 15 W/(m·K)], and the thin ZSM-5 coatings covered on the surface of stainless steel fibers have little effects on the thermal conductivity due to their small thickness (around 4 μm). Therefore, the microfibrous-structured ZSM-5 coating/PSSF catalyst can offer a high thermal conductivity and heat transfer efficiency, leading to smaller temperature gradients and heat transfer limitation in the catalytic structured reactor. Thus, the thermal effects in catalytic combustion reactions of isopropanol over the catalytic structured reactor can be neglected due to the low reactor diameter (10 mm), high gas velocity (30,573 h^{-1} in this study), and relatively high thermal conductivity of modified microfibrous-structured ZSM-5 coating/PSSF catalyst.

Catalytic combustion performance

Catalytic combustion performances of isopropanol over the catalytic structured reactor based on Co–Cu–Mn (1:1:1)/ZSM-5 coating/PSSF catalysts with a bed height of 1 cm (the ZSM-5 coating synthesized at 150°C with a crystallization period of 48 h, the catalyst with a total metal loading of 28 wt % synthesized at a calcination temperature of 350°C) were also investigated using different inlet concentrations of isopropanol (2.1–9.5 mg/L), but at a constant GHSV of 30,573 h^{-1}. Figure 7 shows that some differences of isopropanol conversions can be observed over the catalytic structured reactor under different inlet concentrations of isopropanol. The conversion curves of isopropanol are shifted slightly to higher temperatures as the inlet concentration of isopropanol increased. The $T_{50\%}$ and $T_{90\%}$ (the temperatures at isopropanol conversions approach 50 and 90%) decreased as the isopropanol concentrations decreased. In the case of lower isopropanol concentration (2.1 mg/L), it can be seen in Figure 7 that the complete conversion (100%) of isopropanol was achieved at 300°C. However, for the higher isopropanol concentrations (4.3–9.5 mg/L), the isopropanol conversions cannot reach always 100% at 300°C. The isopropanol conversions at 300°C for different inlet concentrations of isopropanol (4.3, 5.9, 7.2, and 9.5 mg/L) are 99.0, 98.3, 98.1, and 98%, respectively. Therefore, the $T_{100\%}$ (the temperatures at isopropanol conversions approach 100%) increased as the isopropanol concentrations increased. The possible reasons are that the unit catalysts bed in the catalytic structured reactor offers limited active sites for isopropanol combustion and the treated isopropanol quantity in a unit catalysts bed increases at a higher inlet concentration of isopropanol, leading to a decrease in the conversion of isopropanol.[32]

Kinetics modeling for isopropanol catalytic combustion

Considering industrial application of catalyst, it is important to develop a suitable kinetic model with more insights

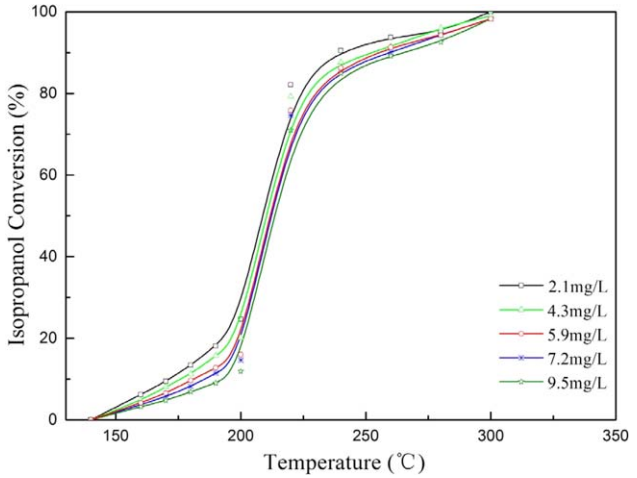

Figure 7. Catalytic combustion performances for isopropanol over the Co–Cu–Mn (1:1:1)/ZSM-5 coating/PSSF catalyst (the ZSM-5 coating synthesized at 150°C with a crystallization period of 48 h, the catalyst with a total metal loading of 28 wt % synthesized at a calcination temperature of 350°C) under different inlet concentrations of isopropanol in the feed stream (2.1–9.5 mg/L, GHSV of 30,573 h^{-1}).

[Color figure can be viewed in the online issue, which is available at wileyonlinelibrary.com.]

into the combustion reaction mechanism of VOCs. In this study, two kinetic models were applied to investigate the catalytic combustion kinetics of isopropanol over the catalytic structured reactor.

Table 1. The Reaction Rates of Catalytic Combustion of Isopropanol over the Catalytic Structured Reactor (Isopropanol Concentration of 2.1–9.5 mg/L, GHSV of 30,573 h^{-1}, Oxygen Concentration of 300.1 mg/L in the Feed Gas)

Inlet Isopropanol Concentration (mg/L)	Reaction Temperature (°C)	Conversion x_i	Reaction Rate [10^{-8} mol/(cm^3 s)]
2.1	160	0.062	2.341
	170	0.094	3.565
	180	0.134	5.077
	190	0.181	6.841
	200	0.247	9.327
4.3	160	0.048	2.894
	170	0.081	4.919
	180	0.112	6.829
	190	0.157	9.549
	200	0.201	12.211
5.9	160	0.041	3.452
	170	0.066	5.466
	180	0.097	8.055
	190	0.128	10.644
	200	0.160	13.320
7.2	160	0.037	3.781
	170	0.057	5.818
	180	0.082	8.348
	190	0.114	11.635
	200	0.147	14.922
9.5	160	0.032	4.333
	170	0.047	6.355
	180	0.069	9.244
	190	0.090	12.133
	200	0.119	16.004

Power–Rate Law Kinetic Model. The power–rate law kinetic model as the simplest kinetic equation can be useful for preliminary kinetic studies and design purposes, but do not provide any insight into the surface reaction mechanism.[34,35,38] For catalytic combustion of VOCs in air, the oxygen concentration in the gas stream is always much higher than that of VOCs.[34] Hence, in this study, the oxygen concentration in the gas steam can be assumed to be constant during the catalytic combustion process of isopropanol over the catalytic structured reactor. The power–law kinetic equation is given by the expression:

$$-r_i = k' C_i^n \tag{3}$$

Equation 3 can be further simplified as:

$$\ln(-r_i) = \ln k' + n \ln C_i \tag{4}$$

where C_i is the concentration of isopropanol, n is the catalytic combustion reaction order, $-r_i$ is the reaction rate [mol/(cm^3 s)], and k is the reaction rate constant.

Mars–Van Krevelen Kinetic Model. Mars–Van Krevelen kinetic model is based on the assumption that catalytic

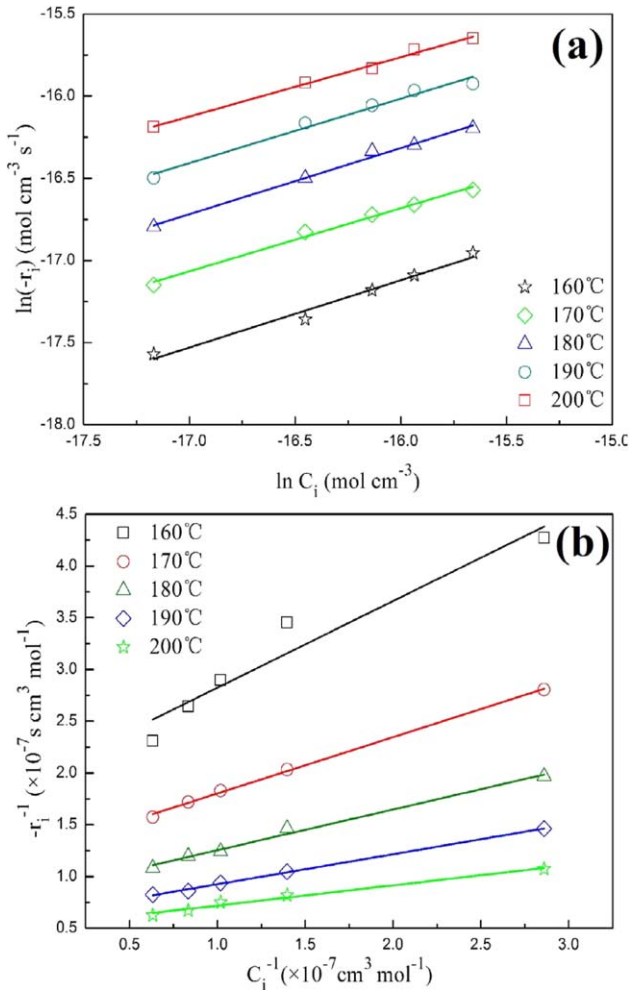

Figure 8. Linear fitting of isopropanol catalytic combustion kinetic data over catalytic structured reactor for the power–rate law model (a), and the Mars–Van Krevelen kinetic model (b).

[Color figure can be viewed in the online issue, which is available at wileyonlinelibrary.com.]

Table 2. Catalytic Combustion Kinetic Parameters of Isopropanol over Catalytic Structured Reactor for the Power–Rate Law Kinetic Model

Power–Rate Law Model	$\ln(-r_i)=\ln k'+n\ln C_i$				
Temperature (°C)	160	170	180	190	200
$\ln k'$	−10.562	−10.534	−9.875	−9.740	−9.972
n	0.410	0.384	0.403	0.392	0.362
k' (s^{-1})	2.259×10^{-5}	2.662×10^{-5}	5.144×10^{-5}	5.888×10^{-5}	4.669×10^{-5}
R^2	0.975	0.989	0.989	0.975	0.992

combustion reaction occurs by interaction between reactant molecule and the oxygen-rich centers of the catalyst.[1,35,38,47,48] The oxygen-rich centers on the catalyst surface could be either chemisorbed or lattice oxygen.[48] Thus, the hypothesis of this model based on an oxidation–reduction mechanism consists of two steps[1,35,38,47,48]:

Step (1): reduction of the oxidized catalyst sites by the VOCs, resulting in oxidation products and reduced catalyst sites

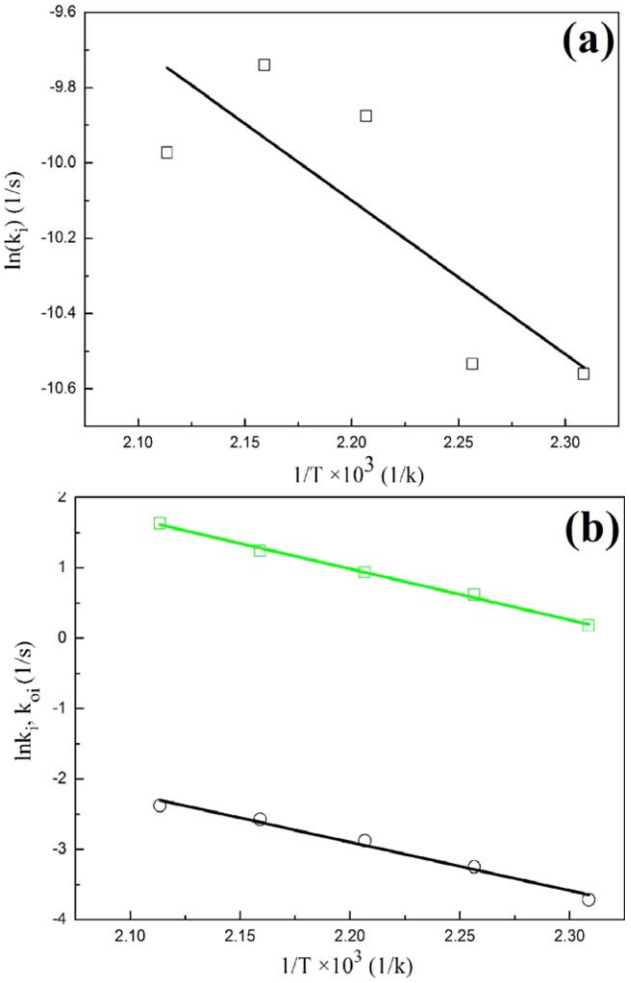

Figure 9. Arrhenius equation fitting of isopropanol catalytic combustion kinetic data over catalytic structured reactor for the power–rate law model (a), and the Mars–Van Krevelen kinetic model (b).

[Color figure can be viewed in the online issue, which is available at wileyonlinelibrary.com.]

$$\mathrm{VOCs+Cat\text{-}O} \xrightarrow{k_i} \mathrm{Cat+CO_2} \tag{5}$$

Step (2): oxidation of the reduced catalyst sites by oxygen from the air to be oxidized catalyst sites again

$$2\mathrm{Cat}+\mathrm{O_2} \xrightarrow{k_{oi}} 2\mathrm{Cat\text{-}O} \tag{6}$$

Hence, the following equations can be derived[41]

$$-r_i = k_i C_i \theta \tag{7}$$

$$-r_{oi} = k_{oi} C_{oi} (1-\theta) \tag{8}$$

where $-r_i$ is the oxidation rate of VOCs, θ is the fraction of activated sites of the oxidized catalyst, C_i is the concentration of isopropanol, $-r_{oi}$ is the oxidation rate of the reduced catalyst, $1-\theta$ is the fraction of reduced sites of the catalyst, and C_{oi} is the concentration of oxygen.

The reaction rates of the two steps should be equivalent at the steady state.[1,35,38,41,47] Thus, if α moles of O_2 ($\alpha = 4.5$, in this study) are required to oxidize 1 mol of VOCs, $-r_{oi}$ should be equivalent to $-\alpha r_i$.[41] According to Gangwal et al.,[49] Eqs. 7 and 8 can be rearranged as following

$$\frac{1}{-r_i} = \frac{\alpha}{k_{oi}C_{oi}} + \frac{1}{k_i C_i} \tag{9}$$

As the oxygen concentration in the gas stream is always much higher than that of VOCs, the $\frac{\alpha}{k_{oi}C_{oi}}$ term can be assumed as a constant λ. Thus, Eq. 9 can be illustrated as following:

$$\frac{1}{-r_i} = \lambda + \frac{1}{k_i C_i} \tag{10}$$

The Arrhenius Equation. It is well known that reaction rate constants obtained from various kinetic models always vary with temperature. The activation energy of the reaction can be calculated using Arrhenius equation, which is given by the expression

$$k = A\exp\left(\frac{-E_a}{RT}\right) \tag{11}$$

where k is the reaction rate constant, A is the frequency factor (s^{-1}), E_a is the reaction activation energy (kJ/mol), R is ideal gas constant [8.314×10^{-3} kJ/(mol K)], and T is the reaction temperature (K).

Table 1 shows the catalytic combustion rates of isopropanol over the catalytic structured reactor, calculated by Eqs. 1 and 2 using the experimental data from Figure 7. First, these data were studied by the power–rate law kinetic model using Eq. 4. Figure 8 presents the linear regression fitting results of these data. According to Eq. 4, the slope of the lines represents the reaction order n and the reaction rate constant k'

Table 3. Catalytic Combustion Kinetic Parameters of Isopropanol over Catalytic Structured Reactor Analyzed by Mars–Van Krevelen Kinetic Model

Mars–Van Krevelen model	$\frac{1}{-r_i} = \lambda + \frac{1}{k_i C_i}\left(\frac{\alpha}{k_{oi} C_{oi}}\right)$				
Temperature (°C)	160	170	180	190	200
$\frac{1}{k_i}$	0.830	0.540	0.390	0.289	0.195
$\frac{\alpha}{k_{oi} C_{oi}} \times 10^{-7}$	1.980	1.250	0.860	0.636	0.523
k_i (s^{-1})	1.205	1.852	2.564	3.460	5.128
k_{oi} (s^{-1})	0.024	0.038	0.056	0.075	0.092
R^2	0.916	0.998	0.988	0.998	0.977

can be calculated from the intercepts of those lines. All the kinetic parameters for the power–rate law kinetic model are summarized in Table 2. Some difference in the reaction order of isopropanol combustion over the catalytic structured reactor at different reaction temperature can be observed in Table 2. Moreover, the reaction rate constant k' does not follow any trend with changes in reaction temperature, indicating that the variation of the reaction rate constants k' with different reaction temperature deviates Arrhenius empiric equation. Figure 9a shows the Arrhenius equation fitting of the reaction rate constants for the power–rate law model, calculating using the kinetic data from Figure 8a and Table 2 and the calculated kinetic data are also summarized in Table 4. As can be seen in Table 2, the value of correlation coefficient R^2 for the rate constants fitting is relatively low (0.563). Above all, it suggests that the power–rate law model does not give a decent fit describing the catalytic combustion kinetic of isopropanol over the catalytic structured reactor.

The experimental data was also investigated by the Mars–Van Krevelen kinetic model using Eq. 9. Figure 8b presents the linear regression fitting results of the kinetic data in Table 1 for the Mars–Van Krevelen kinetic model. The values of k_i and k_{oi} can be calculated using Eq. 9, and all the obtained data are summarized in Table 3. It can be clearly seen in Table 3 that the values of k_i and k_{oi} increase regularly as the reaction temperature increased, indicating that the variation of the reaction rate constants k_i and k_{oi} with different reaction temperature obeys Arrhenius empiric equation. The Arrhenius equation fitting results of the reaction rate constants for the Mars–Van Krevelen model are shown in Figure 9b and Table 4. It can be seen in Table 4 that the reaction activation energies for the reduction and oxidation step are 60.3 and 57.19 kJ/mol, respectively. The values of Pre-exponential factor for the reduction and oxidation steps are 2.28×10^7 and 2.06×10^5, respectively. Moreover, the values of correlation coefficient R^2 for the rate constants fitting are relatively high (0.996 and 0.979). Therefore, it can be concluded that the Mars–Van Krevelen model gives a better fit for describing the catalytic combustion kinetics of isopropanol over the catalytic structured reactor.

Table 4. Catalytic Combustion Reaction Activation Energies (E_a) of Isopropanol over Catalytic Structured Reactor Analyzed by Power–Rate Law Model and Mars–Van Krevelen Kinetic Model

Parameters	Power–Rate Law Model	Mars–Van Krevelen model	
		Reduction	Oxidation
Reaction activation energy Ea (kJ/mol)	33.92	60.30	57.19
Pre-exponential factor A (S^{-1})	0.999	2.28×10^7	2.06×10^5
R^2	0.563	0.996	0.979

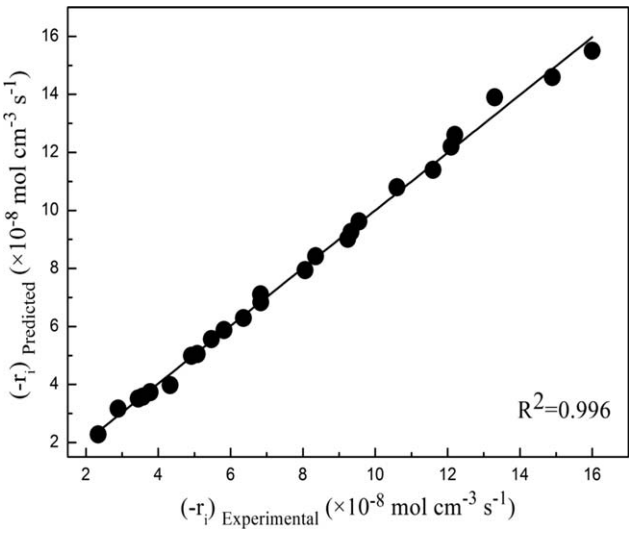

Figure 10. Experimental vs. predicted reaction rates for the isopropanol catalytic combustion over catalytic structured reactor for the Mars–Van Krevelen model (isopropanol concentration of 2.1–9.5 mg/L, GHSV of 30,573 h^{-1}).

Thus, the accuracy of the Mars–Van Krevelen kinetic model was further verified by predicting the reaction rates of isopropanol over the catalytic structured reactor for different inlet concentrations of isopropanol. Figure 10 represents the experimental values of reaction rate vs. the predicted reaction rate values calculated by Mars–Van Krevelen model using Eq. 9. It can be clearly seen in Figure 10 that the predicted reaction rates present a good agreement with the experimental values, giving a relatively high value of correlation coefficient R^2 (0.996). The above results further indicate that the Mars–Van Krevelen Kinetic model can be used to describe the catalytic combustion kinetics of isopropanol at low concentrations in air over the catalytic structured reactor.

As stated above in the assumption of Mars–Van Krevelen kinetic model, the catalytic combustion reaction occurs by interaction between reactant molecule and the oxygen-rich centers of the catalyst. According to our previous report,[32] the H_2-TPR and XPS results (shown in Figures S6 and S8, and Table S2 in Supporting Information) have indicated that the Co–Cu–Mn (1:1:1) mixed oxides modified microfibrous-structured ZSM-5 coating/PSSF catalysts posses many oxygen-rich centers such as Co–Cu–Mn mixed oxides, lattice oxygen and surface oxygen species. It is well known that the oxygen of the catalyst network contributes to the catalytic combustion reaction, and the mobility of this oxygen is very important for catalytic activity of catalyst.[21] As can be seen in Supporting Information, Figure S6, for the Cu–Mn (1:1)/ZSM-5 coating/PSSF catalyst, only one reduction peak can be found at 238°C, attributing to the combined reduction of Cu–Mn mixed oxides. Interestingly, the Co–Cu–Mn (1:1:1)/ZSM-5 coating/PSSF catalyst presents a reduction peak at a lower temperature (around 203°C), which could be attributed to the combined reduction of Co–Cu–Mn mixed oxides. Moreover, the reduction temperature of Co–Cu–Mn

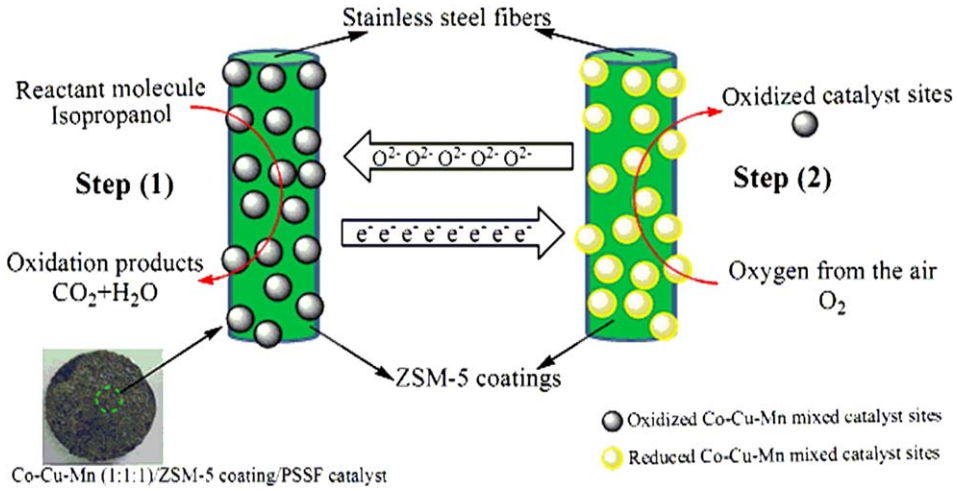

Figure 11. The sketch of catalytic combustion reaction mechanism of isopropanol over the porous microfibrous-structured Co–Cu–Mn (1:1:1)/ZSM-5 coating/PSSF catalyst.

[Color figure can be viewed in the online issue, which is available at wileyonlinelibrary.com.]

(1:1:1)/ZSM-5 coating/PSSF catalysts is much lower than that of Co_3O_4/ZSM-5 catalysts (around 400°C) for propane oxidation,[17] CuO_x/TiO_2 (261 and 305°C) and MnO_x/TiO_2 (417 and 568°C) for toluene oxidation.[21] The H_2-TPR results indicate that the reduction is much easier in the case of the Co–Cu–Mn combinations. Therefore, the mobility of catalyst network oxygen can be enhanced by combination of cobalt–copper–manganese oxides, leading to an improvement of the catalytic activity.[21] Moreover, the XPS results (Figure S8, Table S2 in Supporting Information) indicated that the Co^{3+} and Cu^{2+} were reduced to Co^{2+} and Cu^{1+}, and the Mn^{3+} was oxidized to Mn^{4+} during catalytic combustion process. The reasons are that the Co_2O_3 and CuO species in Co–Cu–Mn mixed oxides maybe the dominating oxidized catalyst sites for the catalytic combustion of isopropanol, however, the Mn species offer smaller catalytic activity for isopropanol oxidation.[32] The XPS results also indicated that the adsorbed oxygen is the main presence form of oxygen, which could be attributed to the high specific surface area and adsorption capacity, and uniform micropore properties of ZSM-5 coating. These excellent properties are also beneficial for the storage enhancement of oxygen and isopropanol species,[30] enormously enhancing the catalytic activity. Thus, on the basis of the above analysis of experimental results and the assumptions of Mars–Van Krevelen model, we propose the mechanism presented in Figure 11 for the catalytic combustion of isopropanol over the Co–Cu–Mn (1:1:1) mixed oxides modified microfibrous-structured ZSM-5 coating/PSSF catalyst. As can be seen in Figure 11, the catalytic combustion reaction occurs by interaction between isopropanol molecule and the oxidized Co–Cu–Mn mixed catalyst sites. Typically, in Step (1), the isopropanol molecule is easily adsorbed onto oxidized Co–Cu–Mn mixed catalyst sites to form an adsorbed compound due to the unique properties of ZSM-5 coating. The adsorbed compound can react with active oxygen in oxidized catalyst sites to produce oxidation products (CO_2 and H_2O) and reduced Co–Cu–Mn mixed catalyst sites. In Step (2), oxygen from the air can be also easily adsorbed onto reduced Co–Cu–Mn mixed catalyst sites to form active oxygen spicies, and then, these active oxygen spicies (O^{2-}) can be transferred from reduced catalyst sites for oxidized catalyst sites to supply the oxygen in catalytic combustion reaction process of isopropanol. In the meantime, the generated electron (e^-) can be also transferred from oxidized catalyst sites for reduced catalyst sites. Thus, the redox reaction repeats to ensure that catalytic combustion reaction of isopropanol proceed over the Co–Cu–Mn (1:1:1) mixed oxides modified microfibrous-structured ZSM-5 coating/PSSF catalyst.

Conclusion

A promising porous thin-sheet cobalt–copper–manganese mixed oxides modified microfibrous-structured ZSM-5 coating/PSSF catalyst was developed by the papermaking/sintering process, secondary growth process, and incipient wetness impregnating method. The resulting catalyst with unique microfibrous structure possess a perfect combination of large void volume, uniform micropore structure, entirely open structure, high thermal conductivity and permeability, thereby leading to a good catalytic activity for isopropanol combustion. Catalytic combustion performances of isopropanol over the catalytic structured reactor based on Co–Cu–Mn (1:1:1)/ZSM-5 coating/PSSF catalysts were investigated for different inlet concentrations of isopropanol. The kinetics study of catalytic combustion of isopropanol over the Co–Cu–Mn (1:1:1)/ZSM-5 coating/PSSF catalysts was carried out using the power–rate law kinetic model and Mars–Van Krevelen kinetic model. The Mars–Van Krevelen kinetic model gave a better fit to explain the catalytic combustion kinetics of isopropanol over the Co–Cu–Mn (1:1:1)/ZSM-5 coating/PSSF catalysts. A catalytic combustion reaction mechanism for isopropanol combustion over the Co–Cu–Mn (1:1:1) mixed oxides modified microfibrous-structured ZSM-5 coating/PSSF catalyst was proposed. The catalytic combustion reaction in the catalytic structured reactor occurred by interaction between isopropanol molecule and the oxygen-rich centers of modified microfibrous-structured ZSM-5 coating/PSSF catalyst. The reaction activation energies for the reduction and oxidation step are 60.3 and 57.19 kJ/mol, respectively.

Acknowledgment

The authors gratefully acknowledge the financial support of the National Natural Science Foundation of China (Nos. 21176086 and 21376101).

Notation

$C_{iso,in}$, $C_{iso,out}$ = inlet and outlet isopropanol concentrations, mg/L
C_{oi} = concentration of oxygen, mg/L
$F_{iso,in}$ = inlet molar flow rate of isopropanol, mol/s
V_{cat} = catalyst volume, cm^3
n = reaction order
$-r_i$ = reaction rate, $mol/cm^3/s$
k, k_i, k_{oi} = reaction rate constant, s^{-1}
T = reaction temperature, K
A = frequency factor, s^{-1}
E_a = reaction activation energy, kJ/mol
R = ideal gas constant, kJ/(mol K)

Greek letters

θ = fraction of activated sites of the oxidized catalyst
α = overall stoichiometry of the reaction

Literature Cited

1. Abdullah AZ, Abu Bakar MZ, Bhatia S. A kinetic study of catalytic combustion of ethyl acetate and benzene in air stream over Cr-ZSM-5 catalyst. *Ind Eng Chem Res*. 2003;42(24):6059–6067.
2. Chen C, Yu Y, Li W, Cao C, Li P, Dou Z, Song W. Mesoporous $Ce_{1-x}Zr_xO_2$ solid solution nanofibers as high efficiency catalysts for the catalytic combustion of VOCs. *J Mater Chem.* 2011;21(34): 12836–12841..
3. Zhang J, Tang X, Dong J, Wei T, Xiao H. Zeolite thin film-coated long period fiber grating sensor for measuring trace organic vapors. *Sens Actuators B*. 2009;135(2):420–425.
4. Beauchet R, Magnoux P, Mijoin J. Catalytic oxidation of volatile organic compounds (VOCs) mixture (isopropanol/o-xylene) on zeolite catalysts. *Catal Today*. 2007;124(3–4):118–123.
5. Beauchet R, Mijoin J, Batonneau-Gener I, Magnoux P. Catalytic oxidation of VOCs on NaX zeolite: mixture effect with isopropanol and o-xylene. *Appl Catal B*. 2010;100(1–2):91–96.
6. Barbero BP, Costa-Almeida L, Sanz O, Morales MR, Cadus LE, Montes M. Washcoating of metallic monoliths with a MnCu catalyst for catalytic combustion of volatile organic compounds. *Chem Eng J*. 2008;139(2):430–435.
7. Azalim S, Brahmi R, Agunaou M, Beaurain A, Giraudon J-M, Lamonier J-F. Washcoating of cordierite honeycomb with Ce-Zr-Mn mixed oxides for VOC catalytic oxidation. *Chem Eng J*. 2013;223: 536–546.
8. Huang Q, Yan XK, Li B, Chen YW, Zhu SM, Shen SB. Study on catalytic combustion of benzene over cerium based catalyst supported on cordierite. *J Rare Earths*. 2013;31(2):124–129.
9. Silva B, Figueiredo H, Santos VP, Pereira MF, Figueiredo JL, Lewandowska AE, Banares MA, Neves IC, Tavares T. Reutilization of Cr-Y zeolite obtained by biosorption in the catalytic oxidation of volatile organic compounds. *J Hazard Mater*. 2011;192(2):545–553.
10. Azalim S, Franco M, Brahmi R, Giraudon J-M, Lamonier J-F. Removal of oxygenated volatile organic compounds by catalytic oxidation over Zr-Ce-Mn catalysts. *J Hazard Mater*. 2011;188(1):422–427.
11. Tian Z-Y, Tchoua Ngamou PH, Vannier V, Kohse-Höinghaus K, Bahlawane N. Catalytic oxidation of VOCs over mixed Co-Mn oxides. *Appl Catal B*. 2012;117:125–134.
12. Joung H-J, Kim J-H, Oh J-S, You D-W, Park H-O, Jung K-W. Catalytic oxidation of VOCs over CNT-supported platinum nanoparticles. *Appl Surf Sci*. 2014;290:267–273.
13. Tidahy H, Siffert S, Wyrwalski F, Lamonier J-F, Aboukaïs A. Catalytic activity of copper and palladium based catalysts for toluene total oxidation. *Catal Today*. 2007;119(1):317–320.
14. Garcia T, Agouram S, Sanchez-Royo JF, Murillo R, Mastral AM, Aranda A, Vazquez I, Dejoz A, Solsona B. Deep oxidation of volatile organic compounds using ordered cobalt oxides prepared by a nanocasting route. *Appl Catal A*. 2010;386(1–2):16–27.
15. Kolodziej A, Lojewska J, Tyczkowski J, et al. Coupled engineering and chemical approach to the design of a catalytic structured reactor for combustion of VOCs: cobalt oxide catalyst on knitted wire gauzes. *Chem Eng J*. 2012;200:329–337.
16. Konova P, Stoyanova M, Naydenov A, Christoskova S, Mehandjiev D. Catalytic oxidation of VOCs and CO by ozone over alumina supported cobalt oxide. *Appl Catal A*. 2006;298:109–114.
17. Zhu Z, Lu G, Zhang Z, Guo Y, Guo Y, Wang Y. Highly active and stable Co_3O_4/ZSM-5 catalyst for propane oxidation: effect of the preparation method. *ACS Catal*. 2013;3(6):1154–1164.
18. Tsoncheva T, Issa G, Nieto JM, Blasco T, Concepcion P, Dimitrov M, Atanasova G, Kovacheva D. Pore topology control of supported on mesoporous silicas copper and cerium oxide catalysts for ethyl acetate oxidation. *Microporous Mesoporous Mater*. 2013;180:156–161.
19. Abdullah AZ, Abu Bakar MZ, Bhatia S. Performance study of modified ZSM-5 as support for bimetallic chromium–copper catalysts for VOC combustion. *J Chem Technol Biotechnol*. 2004;79(7):761–768.
20. Abdullah AZ, Bakar MZ, Bhatia S. Combustion of chlorinated volatile organic compounds (VOCs) using bimetallic chromium-copper supported on modified H-ZSM-5 catalyst. *J Hazard Mater*. 2006; 129(1–3):39–49.
21. Vu VH, Belkouch J, Ould-Dris A, Taouk B. Catalytic oxidation of volatile organic compounds on manganese and copper oxides supported on titania. *AIChE J*. 2008;54(6):1585–1591.
22. Li X, Wang L, Xia Q, Liu Z, Li Z. Catalytic oxidation of toluene over copper and manganese based catalysts: effect of water vapor. *Catal Commun*. 2011;14(1):15–19.
23. Morales M, Barbero B, Cadus L. Total oxidation of ethanol and propane over Mn-Cu mixed oxide catalysts. *Appl Catal B*. 2006;67(3–4):229–236.
24. Tian Z-Y, Bahlawane N, Vannier V, Kohse-Hoeinghaus K. Structure sensitivity of propene oxidation over Co-Mn spinels. *Proc Combust Inst*. 2013;34:2261–2268.
25. Morales MR, Barbero BP, Cadús LE. MnCu catalyst deposited on metallic monoliths for total oxidation of volatile organic compounds. *Catal Lett*. 2011;141(11):1598–1607.
26. Zimowska M, Michalik-Zym A, Janik R, Machej T, Gurgul J, Socha RP, Podobiński J, Serwicka EM. Catalytic combustion of toluene over mixed Cu-Mn oxides. *Catal Today*. 2007;119(1–4):321–326.
27. Li W, Zhuang M, Wang J. Catalytic combustion of toluene on Cu-Mn/MCM-41 catalysts: influence of calcination temperature and operating conditions on the catalytic activity. *Catal Today*. 2008; 137(2):340–344.
28. Liu Y, Wang H, Li J, Lu Y, Xue Q, Chen J. Microfibrous entrapped Ni/Al_2O_3 using SS-316 fibers for H_2 production from NH_3. *AIChE J*. 2007;53(7):1845–1849.
29. Chen H, Zhang H, Yan Y. Preparation and characterization of a novel gradient porous ZSM-5 zeolite membrane/PSSF composite and its application for toluene adsorption. *Chem Eng J*. 2012;209:372–378.
30. Chen H, Zhang H, Yan Y. Novel gradient porous ZSM-5 zeolite membrane/PSSF composite for enhancing mass transfer of isopropanol adsorption in a structured fixed bed. *Ind Eng Chem Res*. 2012; 51(51):16643–16650.
31. Chen H, Zhang H, Yan Y. Adsorption dynamics of toluene in structured fixed bed with ZSM-5 membrane/PSSF composites. *Chem Eng J*. 2013;228:336–344.
32. Chen H, Zhang H, Yan Y. Gradient porous Co-Cu-Mn mixed oxides modified ZSM-5 membranes as high efficiency catalyst for the catalytic oxidation of isopropanol. *Chem Eng Sci*. 2014;111:313–323.
33. Chen H, Zhang H, Yan Y. Catalytic Combustion of volatile organic compounds over a structured zeolite membrane reactor. *Ind Eng Chem Res*. 2013;52(36):12819–12826.
34. Hu C. Catalytic combustion kinetics of acetone and toluene over $Cu_{0.13}Ce_{0.87}O_y$ catalyst. *Chem Eng J*. 2011;168(3):1185–1192.
35. Manta CM, Bozga G, Bercaru G, Bildea CS. Kinetics of o-xylene combustion over a Pt/alumina catalyst. *Chem Eng Technol*. 2012; 35(12):2147–2154.
36. He C, Li P, Cheng J, Hao Z-P, Xu Z-P. A comprehensive study of deep catalytic oxidation of benzene, toluene, ethyl acetate, and their mixtures over Pd/ZSM-5 catalyst: mutual effects and kinetics. *Water Air Soil Pollut*. 2010;209(1–4):365–376.
37. Bedia J, Rosas J, Rodríguez-Mirasol J, Cordero T. Pd supported on mesoporous activated carbons with high oxidation resistance as catalysts for toluene oxidation. *Appl Catal B*. 2010;94(1):8–18.
38. Ordóñez S, Bello L, Sastre H, Rosal R, Díez FV. Kinetics of the deep oxidation of benzene, toluene, n-hexane and their binary mixtures over a platinum on γ-alumina catalyst. *Appl Catal B*. 2002; 38(2):139–149.
39. Barresi AA, Baldi G. Deep catalytic oxidation of aromatic hydrocarbon mixtures: reciprocal inhibition effects and kinetics. *Ind Eng Chem Res*. 1994;33(12):2964–2974.

40. Zhu J, Lars S, Andersson T. Reaction network and kinetics for the catalytic oxidation of toluene over V_2O_5. *J Catal*. 1990;126(1):92–100.
41. Tseng T-K, Chu H. The kinetics of catalytic incineration of styrene over a MnO/Fe_2O_3 catalyst. *Sci Total Environ*. 2001;275(1):83–93.
42. Tseng T-K, Chu H, Ko T-H, Chaung L-K. The kinetic of the catalytic decomposition of methyl isobutyl ketone over a Pt/γ-Al_2O_3 catalyst. *Chemosphere*. 2005;61(4):469–477.
43. Hedlund J, Schoeman BJ, Sterte J. Synthesis of ultra thin films of molecular sieves by the seed film method. *Stud Surf Sci Catal*. 1997; 105:2203–2210.
44. Zampieri A, Dubbe A, Schwieger W, Avhale A, Moos R. ZSM-5 zeolite films on Si substrates grown by in situ seeding and secondary crystal growth and application in an electrochemical hydrocarbon gas sensor. *Microporous Mesoporous Mater*. 2008;111(1):530–535.
45. Hill CG, Root TW. *Introduction to chemical engineering kinetics and reactor design*. New York: John Wiley & Sons, Inc., 2014.
46. Treacy MM, Higgins JB. *Collection of simulated XRD powder patterns for zeolites*, 5th revised ed. Oxford: Elsevier Science Ltd., 2007.
47. Mars P, Van Krevelen DW. Oxidations carried out by means of vanadium oxide catalysts. *Chem Eng Sci*. 1954;3:41–59.
48. Downie J, Shelstad K, Graydon W. Kinetics of the vapor-phase oxidation of toluene over a vanadium catalyst. *Can J Chem Eng*. 1961; 39(5):201–204.
49. Gangwal S, Mullins M, Spivey J, Caffrey P, Tichenor B. Kinetics and selectivity of deep catalytic oxidation of n-hexane and benzene. *Appl Catal*. 1988;36:231–247.

Manuscript received Aug. 13, 2014, and revision received Oct. 11, 2014.